

LASER LINE SCAN CHARACTERIZATION OF GEOMETRIC PROFILES IN LASER METAL DEPOSITION

M. Gegel^{*}, A. Nisbett[†], D. Bristow^{*}, and R.G. Landers^{*}

^{*}Department of Mechanical and Aerospace Engineering, Missouri University of Science and Technology, Rolla, MO 65409

[†]Mechanical Engineering, Georgia Institute of Technology, Atlanta, GA 30332-0405

Abstract

Laser Metal Deposition (LMD) is an additive manufacturing process in which material is deposited by blowing powdered metal into a melt pool formed by a laser beam. When fabricating parts, the substrate is subjected to motion control such that the melt pool traces a prescribed path to form each part layer. Advantages of LMD include relatively efficient powder usage, the ability to create functionally-graded parts and the ability to repair high-value parts. The process, however, is sensitive to variations in process parameters and a need for feedback measurements and closed-loop control has been recognized in the literature [1, 2]. To this end, a laser line scanner is being integrated into an LMD system at the Missouri University of Science and Technology. Measurements from the laser line scanner will provide the feedback data necessary for closed-loop control of the process. The work presented here considers characteristics of the laser line scanner as it relates to scanning LMD depositions. Errors associated with the measurement device are described along with digital processing operations designed to remove them. The parameter bead height is extracted from scans for future use in a closed-loop control strategy.

Introduction

The Laser Metal Deposition (LMD) process consists of blowing powdered metal through a nozzle and into a melt pool that is generated by a laser beam. By moving the substrate relative to the nozzle, continuous lines of material are deposited and parts are built in a layer-by-layer fashion.

The quality and dimensional accuracy of LMD parts are sensitive to numerous processing conditions and variables that are strongly coupled [3, 4]. For example, the heat transfer rate from the melt pool changes throughout the build process, as the part geometry grows and increases in temperature. Wang *et al.* [4] observed a change in melt pool size with layer number. Not only does thermal phenomenon affect melt pool morphology, non-uniform cooling rates across the part can lead to residual stresses that distort part geometry. Variation in part height during a build alters the laser focus and powder catchment efficiency, which influence the rate of material addition. Because it is difficult to predict how these variables change over the duration of a build and there may be unpredictable disturbances, such as fluctuations in the powder feed rate, there is a need for in-process feedback control of laser metal deposition. Feedback control during a build would allow the system to update process parameters as the build progresses and correct for dimensional inaccuracies.

Existing work regarding closed-loop control of LMD includes temperature and height control schemes [5-9]. Of the height control strategies in the literature, the algorithm developed by Sammons [9] is unique because coupling between layers is taken into account by using the principles of repetitive process control. The controller was designed to operate on measurements of the previous layer's bead height. Thus, in order to physically implement the control strategy presented in [9], a suitable device is needed for measuring the height profile in between fabricating each part layer. A laser line scanner is an appropriate instrument for this application because the measurement accuracy is sufficient for characterizing features on the order of magnitude of a melt pool [10]. The particular scanner used in this work is a Keyence LJ-

V7200 which is being integrated into an open-architecture LMD system at the Missouri University of Science and Technology.

The work presented here studies the characteristics of a laser line scanner, particularly with regards to measuring height profiles of LMD deposits. First, a review of laser scanners used in additive manufacturing applications will be provided. Then the functionality of the laser scanner will be described along with typical errors associated with this method of measurement. Next digital processing techniques designed to remove measurement errors such as outliers and noise will be presented. The effectiveness of these digital processing techniques will be demonstrated for scans of a single-layer and multi-layer part. Finally, the cross-section of a single deposited bead will be fit with analytical shapes in order to extract a height parameter for future implementation of closed-loop control.

Literature Review

Others have employed optical techniques to measure height profiles in additive manufacturing. Kummilil *et al.* measured LMD profiles offline using a UBM Microfocus noncontact profilometer [11]. The data exhibited spikes due to the reflectivity of the depositions. The spikes were averaged with several thousand data points to report a single height value for the deposition. Heralić *et al.* [7] used a laser scanner (Micro-Epsilon scanControl 2810-25) and CMOS camera to measure height profiles in a wire-fed laser deposition process. To protect the scanner from high-power laser reflections and heat exposure, the scanner was mounted on a slide that retracted away from the melt pool during deposition. Measurement inaccuracies arose due to the surface being reflective, rounded, and at an elevated temperature. Since the scanner was not intended for measuring hot surfaces, each deposited layer was allowed to cool for 1 min prior to scanning. In another wire-fed deposition process [6], a photodiode and CCD camera were used to measure deposition height in-situ. The scanner diode had a green wavelength of 512 nm to distinguish it from the near-infrared emission of the hot surface. Also the CCD camera had a narrow band-pass filter at the 512 nm wavelength. The scan stripe trailed the GMAW torch by a distance of 17 mm while a tungsten-incandescent cloth served as a barrier between the optical measurement and the melt-pool radiation. The measurement system was calibrated with a stepped aluminum part.

In this work, LMD samples were measured offline. Future work, however, will involve taking scans after each layer is fabricated and using the measurements to update process parameters for the next layer.

Laser Line Scanner

The laser line scanner used in this work was a Keyence LJ-V7200. The main components of the line scanner consist of two lasers with 405 nm wavelengths, focusing lenses, an HSE³-CMOS camera, and a processing chip. To obtain a profile, the scanner projects a laser stripe onto the surface being measured and samples an image of the laser stripe from the CMOS camera. Knowing the distance between the laser source and the camera's focal point, triangulation is employed to calculate the height of the 2D profile illuminated by the laser stripe. Three dimensional scans are generated by repeatedly acquiring 2D height profiles along the length of a scan, labeled as the x direction in Figure 1. This technique has an accuracy on the order of 1 μm , which is appropriate for measuring the morphology of a single bead deposit with dimensions on the order of 1 mm [10]. The laser scanner is also able to cover larger-scale part features on the order 100 mm.

To integrate the laser scanner into an LMD system at the Missouri University of Science and Technology, the scanner was mounted to an Optomec LENS® Print Engine (LPE) as shown in Figure 1. The laser stripe was oriented to scan along the machine's x-axis and the x-axis encoder signal was wired to trigger the scanner's sampling. This allowed for precise spatial intervals between the sampled profiles.

Sampling can be set to occur at any integer multiple of the encoder ticks, which have a resolution of 0.25 μm . Thus, the scan resolution along the x direction is user-defined down to a resolution of 0.25 μm , while the resolution along the y direction is fixed at 100 μm . There exists a trade-off, however, between spatial resolution and scan speed: high resolution scans require slow scan speeds.

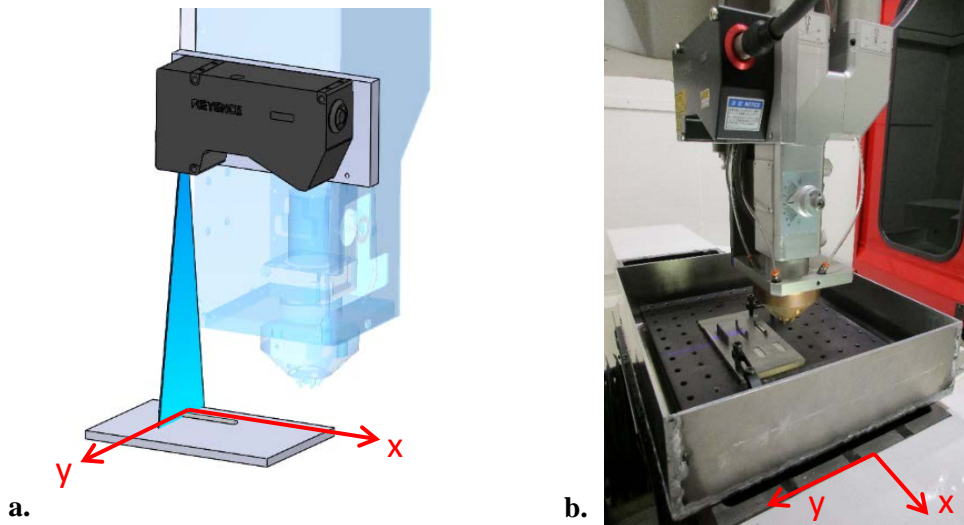


Figure 1: a) Model of laser scanner mounted to LPE and b) photo of laser scanner mounted to LPE.

Sources of error with this measurement technique include occlusions of the camera view and laser projection; specular reflections and multi-reflected light; and noise. Occlusions of the camera view or laser stripe result in unmeasured regions of the part. Stray light due to specular reflections and multi-reflected light poses challenges when measuring reflective surfaces such as LMD parts. To accurately measure the height profile illuminated by the laser stripe, the camera must identify the primary diffuse reflection of the laser stripe for use in the triangulation calculation. If the camera receives specular and multi-reflected light in addition to the primary diffuse reflection, as illustrated in Figure 2a, the sensing unit may not select the primary diffuse reflection for the triangulation calculation, as depicted in Figure 2. Such errors appear as outliers in scan data.

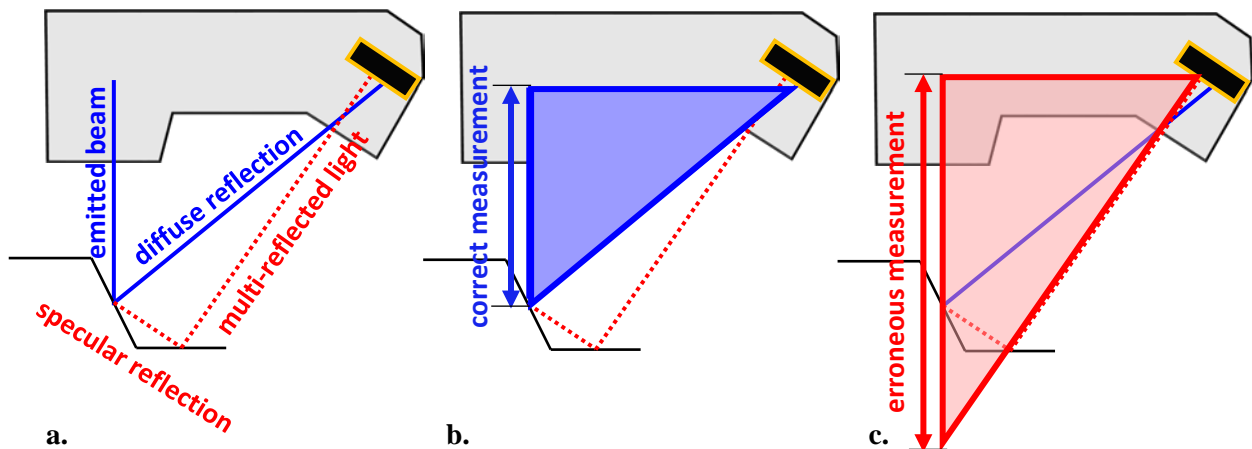


Figure 2: Scanner schematic showing a) paths of the emitted and reflected laser light, b) correct height measurement, and c) erroneous height measurement.

The rest of this paper seeks to remove measurement errors from the scan data in post-processing. An outlier removal method is presented and demonstrated on a scan of a multi-layer stepped part. A 2D smoothing filter is designed to attenuate high-frequency noise and applied to a scan of a single-layer deposition. The effectiveness of both outlier removal and filtering is then quantified by calculating the repeatability of height measurements of an unused substrate. Lastly, a single printed bead is scanned and a bead height parameter is extracted from the data.

Processing Scan Data

The laser line scanner was used to scan the stepped LMD deposit shown in Figure 3. The resulting scan data contained numerous outliers, as shown in Figure 4a. One possible approach to identifying outliers would be to threshold the height and consider all points above the threshold as outliers. This would require knowledge of part geometry because the appropriate threshold value would be location dependent for parts with a range of surface heights, as in the case with the stepped deposit. Instead, the approach applied here takes advantage of the fact the outliers tended to exist as single isolated points or in small clusters and that the height difference between the outliers and neighboring points was larger than the height difference between valid data points. By taking the finite difference, the valid differences in height corresponding to part geometry dropped below the finite difference of the outliers.



Figure 3: Stepped LMD deposit.

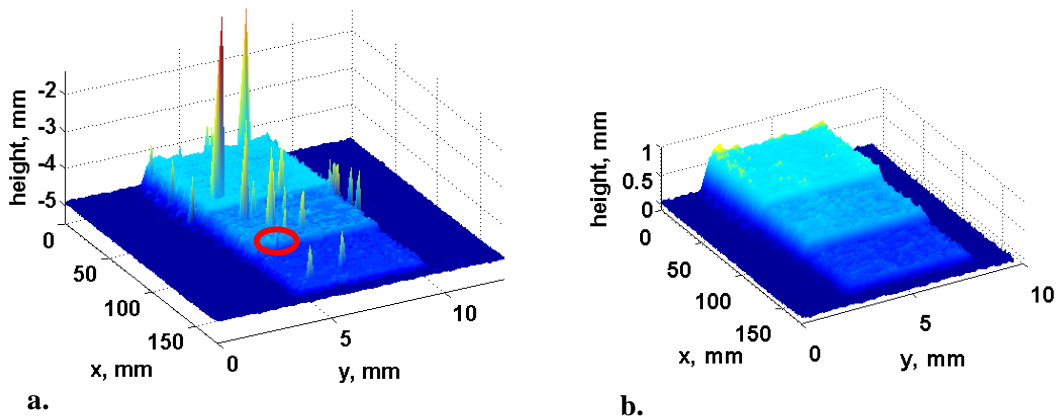


Figure 4: a) Raw scan of stepped deposit and b) scan after outlier removal.

Figure 5a shows a close-up of the region circled in red in Figure 4. The finite difference of this region was taken in Figure 5b. The second level of the stepped part was suppressed in the finite difference operation, although the outliers remained in sharp contrast. Thus, a threshold was uniformly applied to the finite difference at each point, without regard to location. Points above the threshold were identified as

outliers and removed from the data set as shown in Figure 6a. The removed data points were replaced by 2D linear interpolation between neighboring points, which was performed by the Matlab function “griddata.” Figure 6b shows the data after removing outliers. The variance of the points this region was 0.0147mm^2 prior to removing outliers and 0.0115mm^2 afterwards – a decrease of 22%.

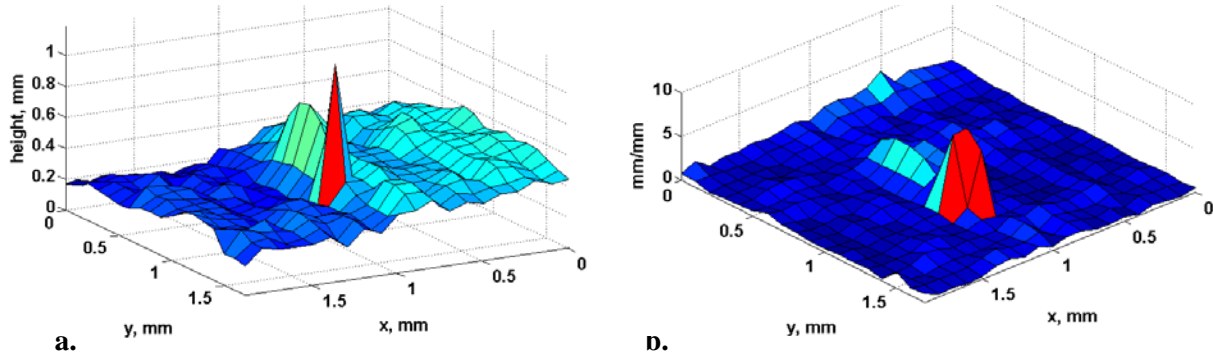


Figure 5: a) Close-up of the region circled in Figure 4 and b) close-up of the finite difference of the region circled in Figure 4.

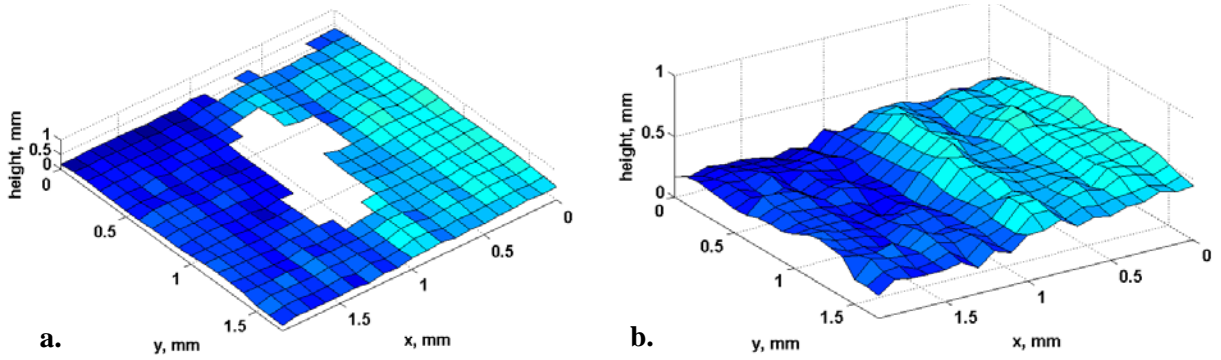


Figure 6: a) Close-up of the region circled in Figure 4 with outliers removed and b) close-up of the region circled in Figure 4 with interpolated points.

In addition to outliers, the raw scan data also contained high-frequency noise. A smoothing filter was designed to remove this high-frequency content. Although digital implementation required a discrete, finite-length filter, the design process began by representing the filter in a spatially-continuous domain. The filter was selected to be a 2D Gaussian of the form

$$h(x, y) = \frac{1}{2\pi\sigma_x\sigma_y} \exp\left(-\left(\frac{x^2}{2\sigma_x^2} + \frac{y^2}{2\sigma_y^2}\right)\right) \quad (1)$$

where h is the filter kernel and σ_x and σ_y are parameters that define the width of the 2D Gaussian in x and y . The frequency response obtained by taking the Fourier transform of (1) is

$$H(f_x, f_y) = \exp\left(-2\pi^2\left(f_x^2\sigma_x^2 + f_y^2\sigma_y^2\right)\right) \quad (2)$$

where f_x and f_y are the spatial frequencies in the x and y directions, having units of mm^{-1} . The value of σ_x was solved from (2) by setting the magnitude of $H(x,y)$ equal to -3dB, specifying the desired cut-off frequency in the x direction and setting $f_y = 0$, which results in

$$\sigma_x = \left(\frac{\ln(\sqrt{2})}{2\pi^2 f_x^2} \right)^{1/2}. \quad (3)$$

The value of σ_y was similarly solved. For this application, the cut-off frequency was selected to be 1 mm^{-1} because that corresponds to the approximate size of an LMD melt-pool, which is assumed to be the fundamental size of printed features. The filter was digitally implemented by sampling the continuous-domain kernel over a finite interval, as expressed by

$$h(n_x dx, n_y dy) = \frac{1}{2\pi\sigma_x\sigma_y} \exp\left(-\left(\frac{(n_x dx)^2}{2\sigma_x^2} + \frac{(n_y dy)^2}{2\sigma_y^2}\right)\right) \quad (4)$$

where dx and dy are the scan resolutions in the x and y directions, N_x and N_y are odd integers corresponding to the numbers of samples in the x and y directions of the filter, and n_x and n_y are integers within the ranges

$$\begin{aligned} -\frac{1}{2}(N_x - 1) &\leq n_x \leq \frac{1}{2}(N_x - 1) \\ -\frac{1}{2}(N_y - 1) &\leq n_y \leq \frac{1}{2}(N_y - 1). \end{aligned}$$

The parameters N_x and N_y represent the number of elements in the x and y directions, respectively, of the 2D filter. The value of N_x was chosen as the ceiling of $6\sigma_x$, or $\lceil 6\sigma_x \rceil$ and N_y was similarly selected.

The sample in Figure 7a was scanned with resolutions in the x and y directions of 6 and 100 μm , respectively. The results of filtering are shown in Figure 7b. Qualitatively, high-frequency noise appears absent from the filtered data.

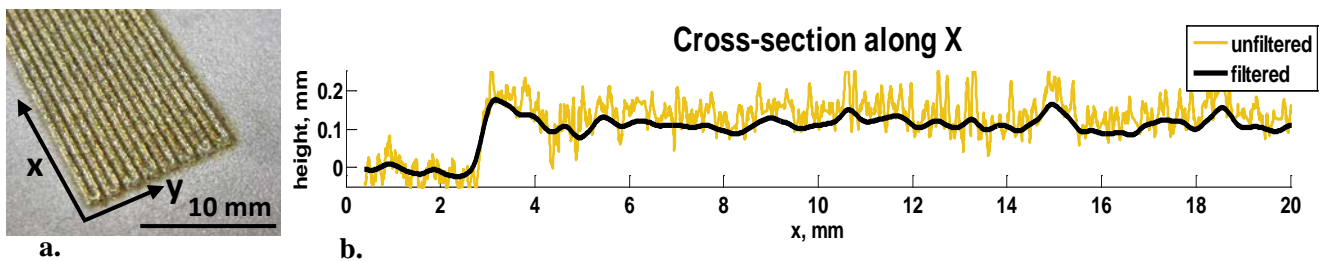


Figure 7: a) Sample scanned with different resolutions in x and y directions and b) filtered and unfiltered data for a cross-section along x direction.

To quantify the effectiveness of outlier removal and smoothing, the repeatability of scan measurements was evaluated with and without digital processing. The same region of an unused substrate was scanned three times and the variation between repetitions was quantified with the 3σ value. Table 1

shows the 3σ values for the raw and processed scans. Since outliers are infrequent compared with number of data valid points over this region, removing outliers significantly reduced the maximum 3σ and yet had little effect on the mean of the 3σ values. Filtering served to reduce both the maximum and mean 3σ values by a factor of 3. Overall, processing was found to improve the repeatability by a factor of about 6 in terms of maximum 3σ . Figure 8 displays graphically the spatial distribution of the 3σ values. Interestingly, in Figure 8a the central region of the scan stripe appears less repeatable than the edges. This is likely due to the larger angle of incidence between the laser and the substrate near the center of the scan stripe.

Table 1: 3σ values for the raw and processed scans.

	Raw Scan	Outliers Removed	Outliers Removed and Filtered
Maximum (mm)	0.591	0.371	0.098
Mean (mm)	0.069	0.068	0.022

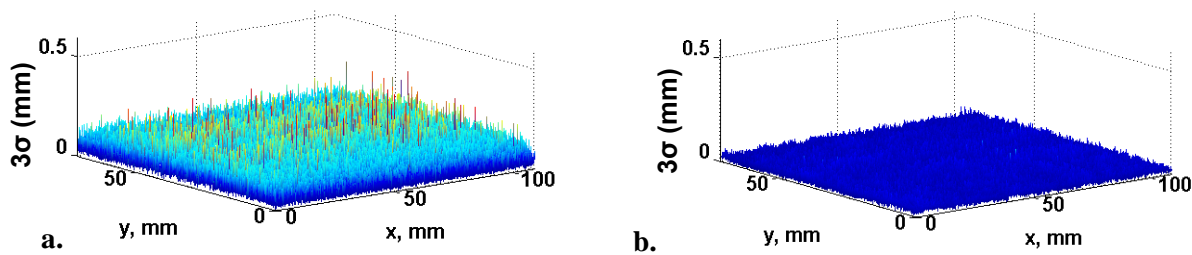


Figure 8: Spatial distribution of 3σ values for unused substrate: a) raw scan data and b) processed scan data.

After removing outliers and filtering the scan data, the parameter of bead height was extracted for future work in implementing closed-loop control. This was accomplished by fitting analytical shapes to cross-sections of the single bead deposit shown in Figure 9.

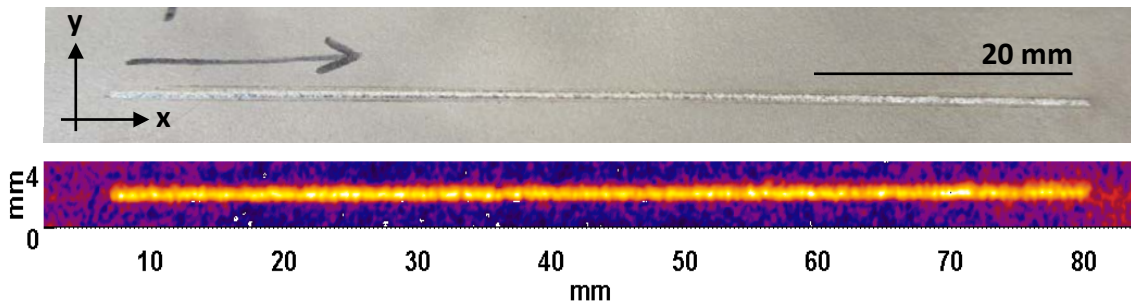


Figure 9: Photo (top) and scan (bottom) of single bead deposit used in extracting height parameters.

A Gaussian curve was fit to each cross-section along the bead's length using the "fit" function in Matlab. A representative cross-section is given in Figure 10, where the height is labeled as the peak value of the Gaussian and the width is considered to be the length of the interval $(-3\sigma, 3\sigma)$. The height fitted at each cross-section is plotted along the length of the bead in Figure 11 and the width is shown in Figure 12. In future work, the extracted height will be fed back into the control algorithm developed in [9].

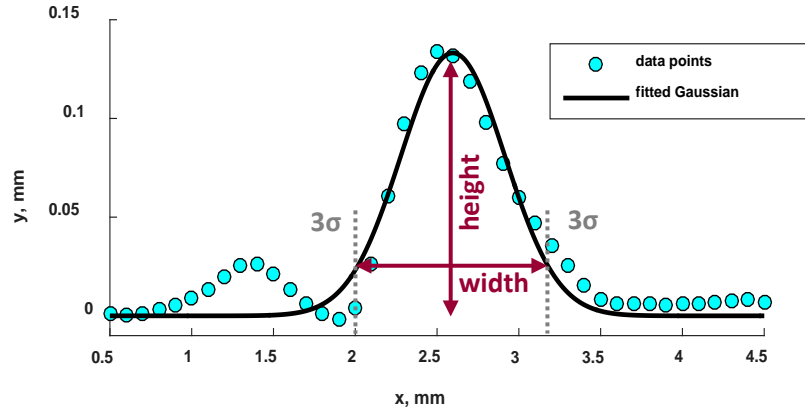


Figure 10: Measured cross-section of bead plotted with fitted Gaussian.

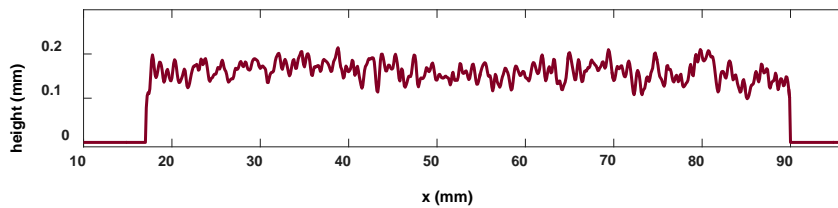


Figure 11: Fitted height along bead in the x direction.

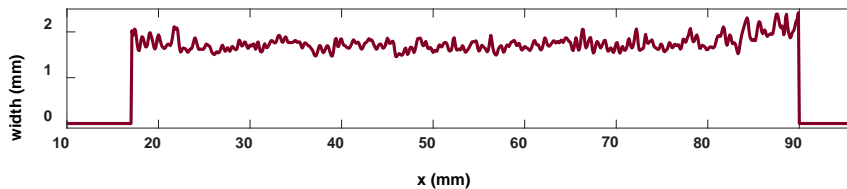


Figure 12: Fitted width along bead in the x direction.

Summary, Conclusions and Future Work

Layer-by-layer feedback measurements of LMD builds are desirable for use in closed-loop control schemes. Laser line scanners have the ability to measure with the accuracy necessary for capturing deposited features. To this end, the work presented here seeks to evaluate the measurement characteristics of a laser line scanner for future implementation of feedback control.

Raw scans from the laser line scanner contain measurement errors such as outliers and noise. If the outliers consist of single, isolated points or small clusters, then an effective method of outlier identification consists of taking the finite difference and applying a threshold. A 2D smoothing filter was applied to remove high-frequency noise. Both the outlier removal and filtering processes were found to improve the repeatability of scan measurements by a factor of approximately 6.

To extract the parameter of bead height, Gaussian curves were fit to each cross-section along the length of a deposit. This was done for a straight, single-bead deposit. Since part layers will not always consist of straight lines, the fitting operation will need to be modified to handle curved depositions. The

height parameter extraction will also need to accommodate the case of side-by-side overlapping tracks, where the cross-sectional shape cannot be sufficiently captured using a Gaussian curve.

Acknowledgements

The authors would like to acknowledge Lucas Brewer, Berto Chavez, and Justin Vollbrecht at Optomec for their expertise and use of equipment; and Joseph Drallmeier at Missouri S&T for contributions to the fabrication of the LMD system. This project receives funding through GAANN (P200A150309) and NSF (CMMI 1301414), as well as the Center for Aerospace Manufacturing Technologies and the Chancellor's Distinguished Fellowship at the Missouri University of Science and Technology.

References

- [1] Y. Huang, M. C. Leu, J. Mazumder, and A. Donmez, "Additive Manufacturing: Current State, Future Potential, Gaps and Needs, and Recommendations," *Journal of Manufacturing Science and Engineering*, vol. 137, p. 014001, 2014.
- [2] I. S. D. a. NIST, "Measurement Science Roadmap for Metal-Based Additive Manufacturing," May 2013.
- [3] K. Zhang, S. Wang, W. Liu, and X. Shang, "Characterization of stainless steel parts by Laser Metal Deposition Shaping," *Materials and Design*, vol. 55, pp. 104-119, 2014.
- [4] L. Wang, S. D. Felicelli, and J. E. Craig, "Thermal modeling and experimental validation in the LENS TM process," *18th Solid Freeform Fabrication Symposium, Austin, TX, 2007*, pp. 100-111.
- [5] L. Tang and R. G. Landers, "Melt Pool Temperature Control for Laser Metal Deposition Processes—Part I: Online Temperature Control," *Journal of Manufacturing Science and Engineering*, vol. 132, p. 011010, 2010.
- [6] C. Doumanidis and Y.-M. Kwak, "Geometry Modeling and Control by Infrared and Laser Sensing in Thermal Manufacturing with Material Deposition," *Journal of Manufacturing Science and Engineering*, vol. 123, p. 45, 2001.
- [7] A. Heralić, A.-K. Christiansson, and B. Lennartson, "Height control of laser metal-wire deposition based on iterative learning control and 3D scanning," *Optics and Lasers in Engineering*, vol. 50, pp. 1230-1241, 2012.
- [8] A. Fathi, A. Khajepour, E. Toyserkani, and M. Durali, "Clad height control in laser solid freeform fabrication using a feedforward PID controller," *The International Journal of Advanced Manufacturing Technology*, vol. 35, pp. 280-292, 2006.
- [9] P. M. Sammons, D. A. Bristow, and R. G. Landers, "Repetitive Process Control of Laser Metal Deposition," ASME Dynamic Systems and Control Conference, San Antonio, TX, 2014.
- [10] J.-A. Beraldin and M.-A. Drouin, "Active 3D Imaging Systems," in *3D Imaging, Analysis and Applications*, N. Pears, Ed., ed: Springer, 2012.
- [11] J. Kummailil, C. Sammarco, D. Skinner, C. A. Brown, and K. Rong, "Effect of Select LENS™ Processing Parameters on the Deposition of Ti-6Al-4V," *Journal of Manufacturing Processes*, vol. 7, pp. 42-50, 2005.